AIAA SciTech Forum
January 3-7, 2022, San Diego, CA & Virtual
AIAA SCITECH 2022 Forum

10.2514/6.2022-0076

In-Situ Monitoring of Additive Manufacturing using Digital Image Correlation

Martina Jani[1], Sandeep Chava[2], Jeff Brown[3] , and Sirish Namilae[4]*
Embry-Riddle Aeronautical University, Daytona Beach, FL, 32114, USA

Advances in additive manufacturing over the past decade have led to its applications in multiple fields. Additive manufacturing answers the need for high flexibility in designing complex structures, however, the rapid thermal fluctuations during processing lead to numerous defects and processing-induced residual stresses. In this research, an in-situ approach using Digital Image Correlation (DIC) is developed to monitor the deformation during the processing, and thereby analyze the formation of defects. DIC is an optical technique that compares the changes in the grey value pattern of a printed speckle pattern in consecutive images of a specimen to determine the displacements and strains. The infrared thermal camera is used to correlate deformations to thermal history. Results on a thermoplastic specimen with pre-printed speckles show how strain is continuously varying throughout the printing process. Further defects like warpage and layer deposition are correlated to the change in strain evolution. Thermal analysis of the specimen during processing illustrates temperature variations during the printing process.

I. Nomenclature

ϵ_{xx}	=	strain in the X direction
ϵ_{yy}	=	strain in the Y direction
Smn	=	sections within a 3D printed layer
L1	=	layer one of the three-layer sample
L2	=	layer two of the three-layer sample
L3	=	layer three of the three-layer sample

II. Introduction

Additive manufacturing builds solid parts based on the designed model through the layer-by-layer deposition of material [1]. Several advantages such as reduced manufacturing cost, process time, material wastage, easy recycling, and remanufacturing have captivated the attention of aerospace, biomedical, and transportation industries. It is also advantageous in terms of design flexibility, weight reduction, and improved functionality of the manufactured components [2]. Additive manufacturing is interchangeably called rapid prototyping due to its former primary purpose to rapidly replicate designed models. However, additive manufacturing now has evolved from its role of mere prototyping technique to direct manufacturing process [3].

The aerospace industry is the fourth highest consumer of additive manufacturing technology with applications such as additively manufactured cobalt nozzles (GE aviation), thermoplastic parts (Boeing), engine prototyping (Hindustan Aeronautics Limited), rocket engine igniter (NASA), etc. [4]. Airbus used these concepts to manufacture an aluminum part for Eurostar E3000, which weighs 35% less while increasing the stiffness by 40% [5]. In 2014, NASA sent a zero-gravity 3D Printer based on fused deposition melting (FDM) technology on International Space

[1] Graduate Student, Department of Aerospace Engineering (Martina.Jani@my.erau.edu).
[2] Graduate Student, Department of Aerospace Engineering (Sandeep.Chava@my.erau.edu).
[3] Professor, Department of Civil Engineering (Jeff.Brown@erau.edu).
[4] Associate Professor, Department of Aerospace Engineering (Sirish.Namilae@erau.edu) (*Corresponding Author).

Station, which successfully collected printed tensile, compression, flexural and other mechanical test coupons to further investigate their characters from the microgravity environment [6]. Industrial sectors such as biomedical, architectural, and automotive employ additive manufacturing for drug development, non-bioactive implants, architectural modeling, customized car seats, car chassis, etc. [1,7,8]. Recently, 3D printed personal protective equipment kits, isolation chambers, COVID-19 specimen collectors, and ventilators aided significantly to mitigate emergencies that arose during this pandemic [9].

In the aerospace industry, components with complex designs can be easily manufactured with lightweight materials using additive manufacturing techniques [10]. Designs with reduced use of fasteners and rivets, as well as faster production of customized single-use parts are possible through these methods [10-12]. Despite these advantages manufacturing defects due to Poor bonding between printed layers, high porosity, poor surface finish, oozing effect, wall gaps, missing material, dimensional inaccuracies, residual stress due to non-uniform cooling, and post-processing requirements have limited its expanded use [3,11–13].

Consequently, many researchers have recently attempted to monitor additive manufacturing using in-situ methods so that defect formation can be proactively mitigated. Optical techniques involving the use of charged-coupled device (CCD) camera, high-speed camera, and infrared (IR) camera are some of the popular in-situ techniques. Optical monitoring using laser for layer-wise laser melting process to detect defects in actual time was implemented by Craeghsa et al. [14]. A unique method called "mapping of pool data" enabled mapping melt pool data in space, simultaneously with mapping laser beam position. They have considered the effect of temperature on inducing thermal stresses during selective laser melting and found out that overhang zones experience overheating which caused deformation.

Kousiatza et al. [15] developed a Fiber Bragg Grating (FBG) sensor to obtain in-situ real-time monitoring of strain and temperature variation in additive manufacturing. They observed a change in residual strain values based on specimen position on the print bed. Vanaei et al. developed an in-situ temperature measurement technique during fused deposition modeling of PLA [16]. They considered the sensitivity of thermal energy for each layer of the part based on platform temperature and print speed. They also identified that print speed also influences the rate of cooling and these analyses can further help to detect defects based on improper bonding influenced by thermal energy.

Digital Image Correlation (DIC) was first introduced by W.H. Peters & W.F. Rafson in 1982 for stress analysis [17]. It is an optical non-contact method that can measure full-field displacement and strain on a specimen without damaging it. DIC works on the principle of capturing and comparing, the original and deformed image, which is captured after a certain period by dividing it into a subset of pixels. This subset is matched in all the images captured after the reference image to track the displacement of those pixel positions [18]. DIC technique offers several benefits over conventional strain measurement techniques. Firstly, there is no possibility of damaging the specimen, as DIC is a non-contact method to gauge strain. Strain can be observed in three dimensions instead of focusing on one direction [19]. Full-field strain evolution can be obtained using DIC instead of strain at selected points [20]. The major limitation of the conventional strain gauge is that it is limited to certain shapes when it comes to strain measurement and can only be used once at a time. The DIC system overcomes this limitation while taking less time to set up and test as compared to extensometer placement [21].

DIC is extensively used for measuring in-plane strain during tensile testing of material in the literature [22–25]. Plastic zone of low carbon steel specimen was observed using DIC under uniaxial test and true stress-strain curves were obtained [26]. It was noticed that the region that has not entered the plastic zone stays in a constant deformed zone and the region that is in process of entering the plastic zone demonstrates axial plastic deformation due to displacement of the testing machine. DIC is not limited to tensile tests, Górszczyk et al. successfully carried-out testing of coupons made from rock, soil, HMA (Hot-Mixed Asphalt), and geogrids under compression, bending, and indirect tensile tests [21]. Chava et al. used DIC to obtain residual stress evolution on composite with symmetric and asymmetric layups and accounted for dimensional inaccuracy during the cure cycle [27]. All these applications of DIC from the literature show its potential to be considered as an in-situ technique in additive manufacturing.

Even though additive manufacturing has various advantages, its limitations hinder wider application for heavy-duty components. Poor bonding of layers, presence of pores, poor surface finish, oozing effect, wall gaps, missing material, dimensional inaccuracies, residual stress due to non-uniform cooling, and post-processing requirements make it less efficient [3,11–13]. These defects are a function of various print parameters such as infill pattern, infill density, print speed, extruder temperature, platform temperature, filament material. Numerous researchers from the literature analyzed different manufacturing parameters like layer resolution, temperature, and other variables to obtain better surface finish and mechanical properties [3,28,29] but in-situ experimental approaches that identify the defect initiation are limited.

To better understand the mechanics for the formation of defects, it is necessary to monitor the initiation and development of defects during 3D printing through in-situ monitoring of the printing in real-time. In-situ processes

such as Fiber Bragg Grating (FBG) sensors and high-speed cameras were utilized to monitor the manufacturing processes [14,30,31]. While incorporating FBG sensors during additive manufacturing is challenging, the lack of extensive post-processing analysis made high-speed cameras inadequate. DIC overcomes these limitations and has been recently used for real-time observation of strain evolution of composite plies during curing as a part of the conventional manufacturing process [32]. In this research, the objective is to adapt the DIC approach to identify the development of defects and demonstrate its potential as an in-situ technique in additive manufacturing. While the preliminary application is for PLA, the approach developed here could be easily extended to other materials.

III. Experimentation

A. Material, Equipment, and Software

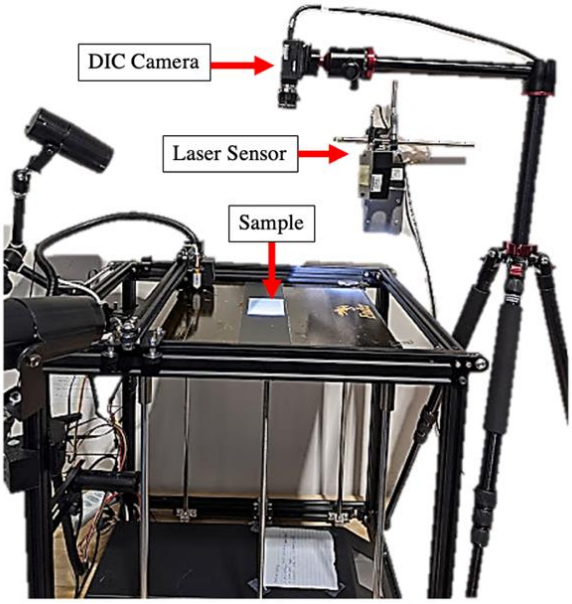

Fig. 1 Experimental DIC system setup

A Marble PLA filament with a black and white pattern on filament procured from Enotepad is used in this research with recommended print and platform temperature ranges from 200-230°C and 60-80°C respectively. Differential Scanning Calorimetry (DSC) enables physical properties of a material based on its property changes with respect to temperature. The melting point for PLA was obtained using DSC. Based on an average of two tests, the melting point of the sample is between 150°C and 160°C. Creality Ender 5 Plus 3D printer is used for printing in this research. It is FDM type printer with a print accuracy of +/-0.1 mm. The outer frame structure of the printer makes it convenient to set up the DIC camera around it. Creality slicer 4.8.0 software is used to convert the CAD model to G-code, which guides machine tool movements in the print direction. Print variables like layer height, print speed, print temperature, and various print-related settings can be updated using this slicer.

DIC camera with an in-plane resolution of 0.00002*FOV and strain range 0.010% to >2000 % has been used along with a lens of 50 mm focal length. The DIC system, VIC-Snap acquisition software, and VIC-2D analysis software from Correlated solutions are used to acquire and analyze captured images. Laser displacement sensor encompasses position sensitive device and laser light-emitting source and measures the thickness, height, vibration of the target object. In this research laser, displacement sensor measures the layer thickness of the PLA sample to verify the print accuracy. An infrared (IR) camera captures the temperature of the object based on the infrared energy intensities of the heat-emitting object. FLIR A655 SC is used to capture the temperature and cooling rate of parts in real-time. This IR camera can capture a temperature range from -40°C to 650°C with an accuracy of +/- 2% and a resolution of 640x480 with an f-number value of one. Research IR software allows post-processing of the thermal images.

B. Setup and Print Algorithm

The experimental setup can be seen in Fig.1, with the DIC system leveled on top of a 3D printer to capture the whole specimen. It is challenging to capture specimens throughout the printing process as the extruder and its channel blocks the full view of the specimen while being printed. Therefore, an algorithm has been developed and implemented which divides each layer of the rectangular specimen (96mm*60mm) into three sections as shown in Fig. 2. Extruder moves out of camera's field of view for 5 seconds after printing each section of the layer to capture the images. This algorithm allows surveillance of the progression of defect formation throughout the layer. G-code, which controls the motion of the print head of the printer, is modified such that it dwells for the desired period with no extrusion. The in-situ method developed in this research is used to monitor flat rectangular specimens with three printed layers.

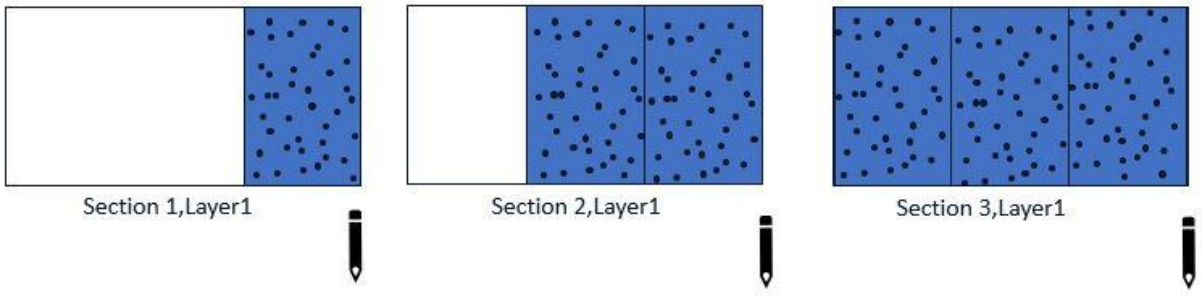

Fig. 2 Print sequence

IV. Experimental Results & Discussion

A. DIC Strain Analysis

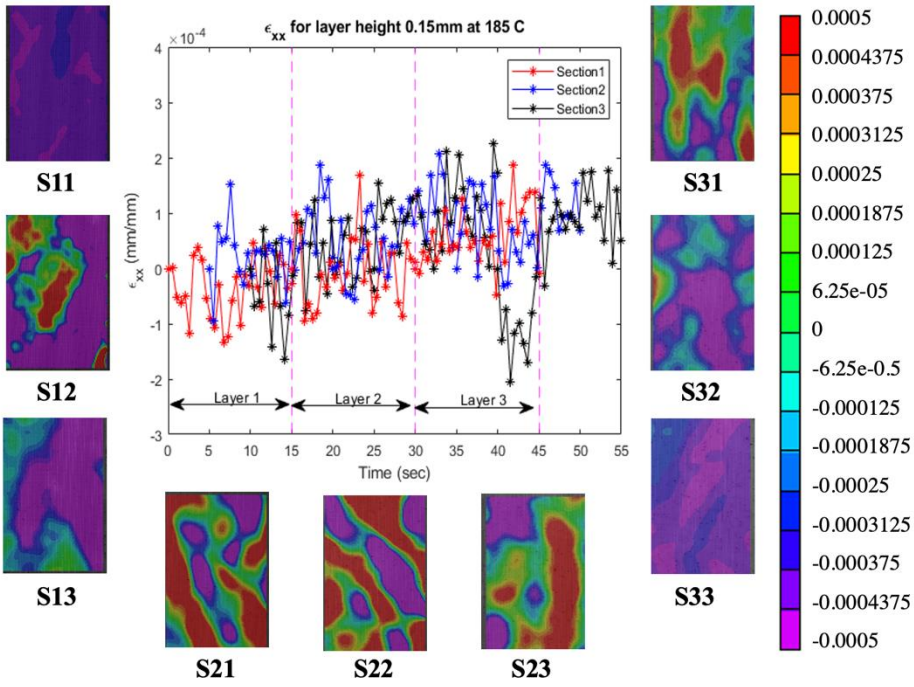

Fig. 3 Strain evolution in X-Direction

The DIC images are analyzed for change in strain according to layers and their sections. Each printed section of a given layer is analyzed while the next two sections of the layer were being printed. Figures 3 and 4 show the strain evolution in X and Y directions for all the layers of the sample respectively. The sample is printed with the following print parameters: print temperature of 185C, print speed of 60mm/s, and a layer thickness of 0.15 mm. The red line in these figures indicates the strain evolution of section 1 in all three layers. The blue and black lines indicate the strain

evolution of section 2 and section 3 respectively. The strain contours (Smn) can also be observed in these figures with 'm' representing the layer and 'n' representing the section of that layer. For example, contour S11 is the strain contour after printing section 1 of layer 1. It can be observed from Fig. 3 that strain in the X direction (ϵ_{xx}) for all three sections increased throughout the printing process as the material is shrinking while it is being cured. The strain in section 3 of layer 3 (S33) is lower due to the presence of an under extrusion as seen in Fig. 5.

The continuous evolution of strain in the Y direction (ϵ_{yy}) can be seen in Fig. 4. Like the strain evolution in the X direction, the strain in the Y direction increases in the first two layers for all three sections. It can also be observed that strain along the Y direction ranges from -2.17E-4 to 2.55E-4 and in the X direction, it ranges from -2.04E-4 to 3.24E-4 indicating that the strain range along the X direction is 21% higher than in the Y direction. This increase can be attributed to the unidirectional print algorithm printing the sample only in the Y direction as seen in Fig. 5. This higher strain in the X direction can be related to the higher expansion of the specimen in this direction to bind with adjacent sections. The increment in Y strain can be related to the tendency to bind with the boundary, which is printed before printing each layer. Also, as the under extrusion shown in Fig. 5 is in parallel to the Y direction, its effect cannot be seen in Fig. 4. These results show the potential of this experimental setup to detect defects irrespective of their location within the sample.

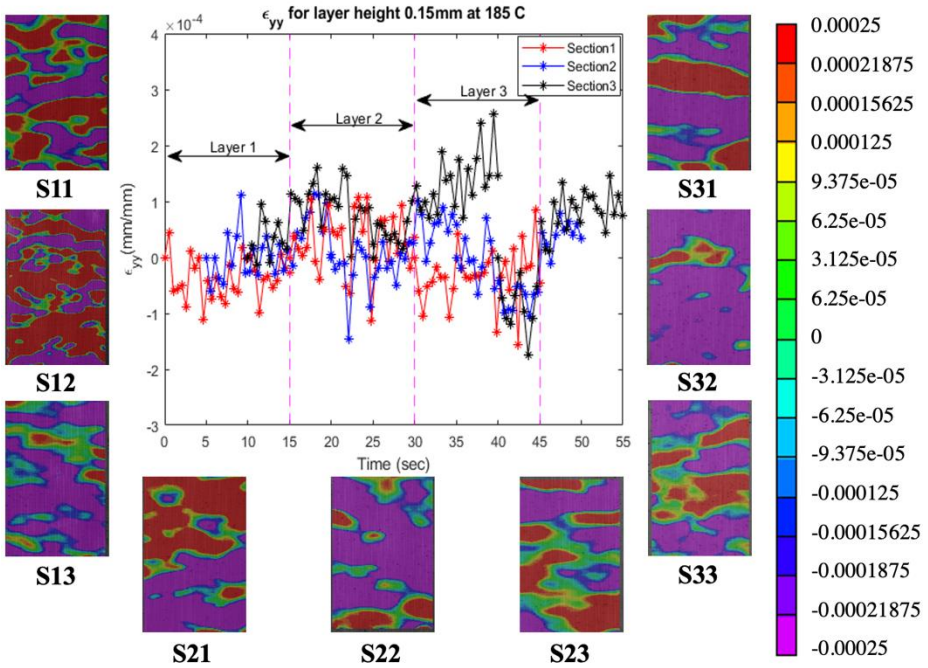

Fig. 4 Strain evolution in Y-Direction

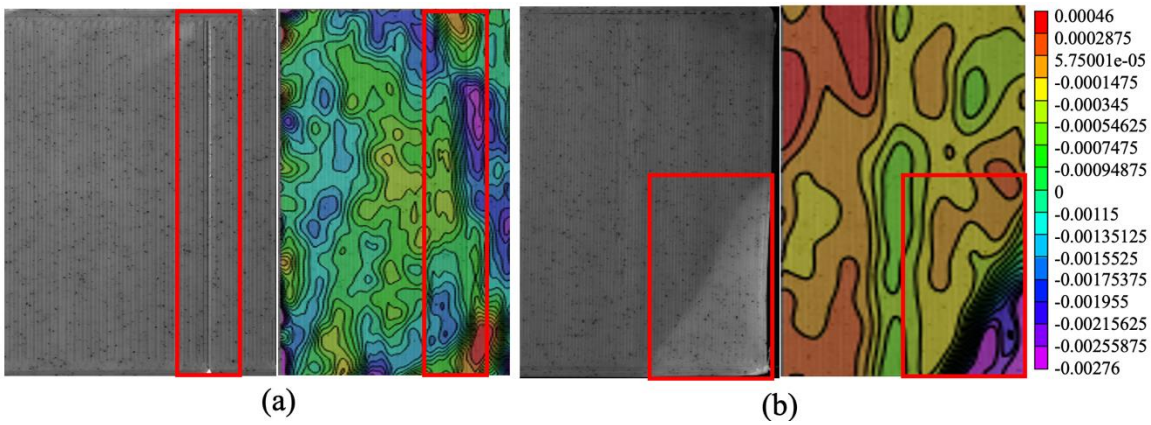

Fig. 5 (a) Under extrusion captured by DIC (b) Warping captured by DIC

B. Defect Characterization

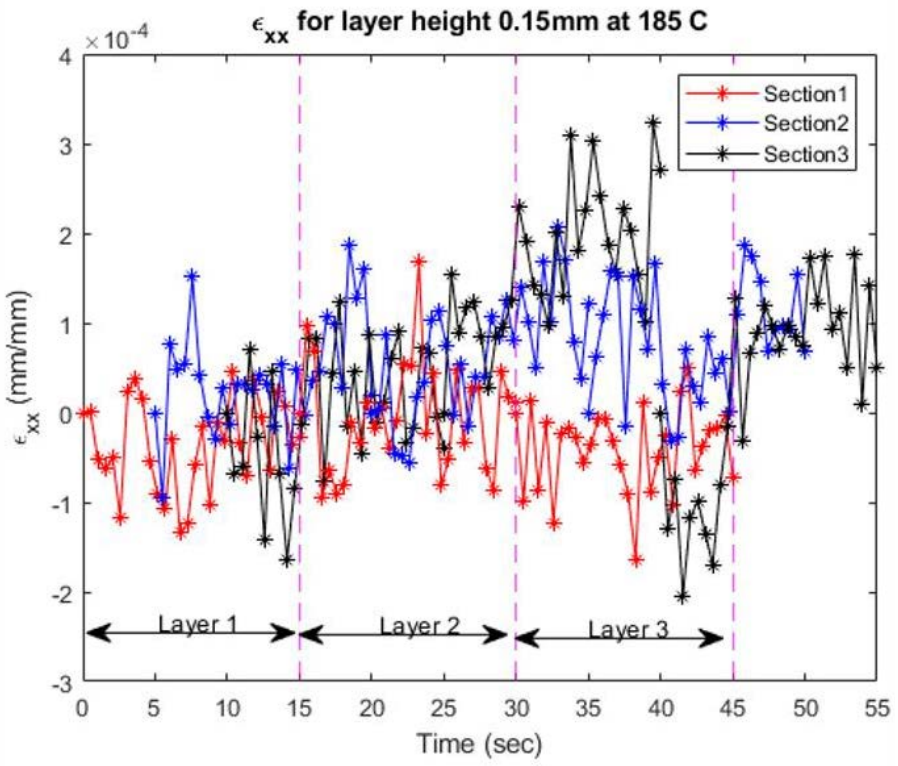

Fig. 6 Compressive strain in section S31 along X-Direction

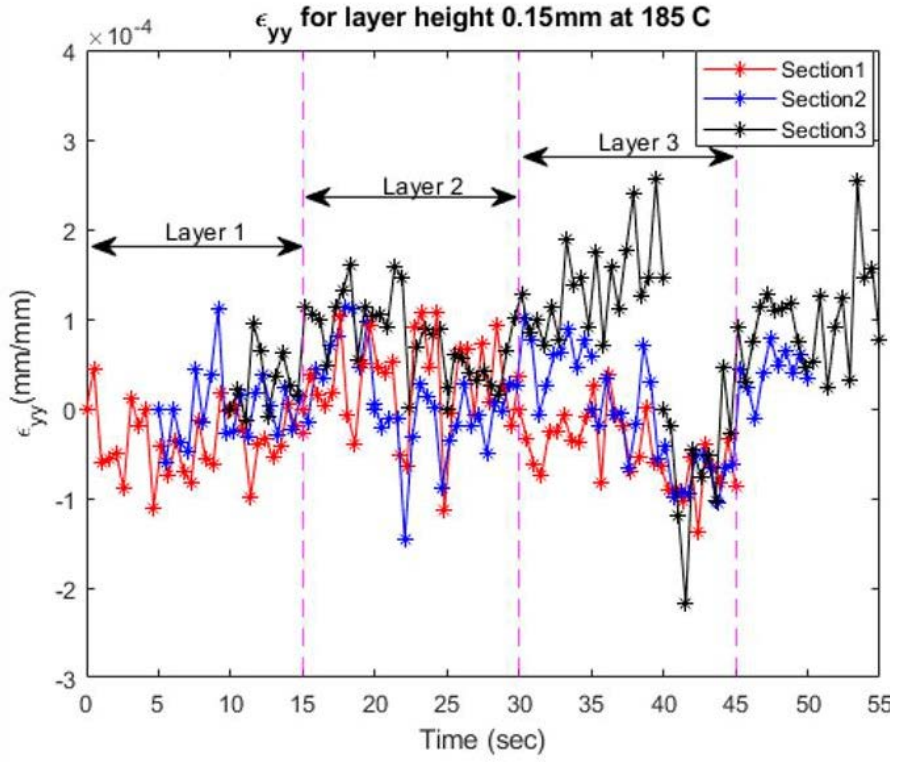

Fig. 7 Compressive strain in section S31 along Y-Direction

Warping is another commonly observed phenomenon in 3D printed parts due to the rapid cooling of material deposited on the platform, which causes the material to shrink and raise from the print platform. Several factors such as speed of the cooling fan, absence of raft, and poor deposition of material on print bed associated with printing initiate warpage. External factors like surrounding temperature and airflow can also alter print quality. Among all these factors, the prominent factor for warpage is insufficient to print platform temperature. In this research, the platform temperature was set to 60°C as recommended by the PLA manufacturer. However, when the experimental setup is moved next to a frequently used exit, the warping defect is identified in a section along the edge of the print platform. Real-time monitoring of sample while printing enabled capturing this phenomenon in the final layer final section as seen in Fig. 6 and Fig. 7. The warpage defect is usually identified after printing the sample as seen in Fig. 5 but with continuous evolution using DIC used in this research, it is possible to detect the exact starting point of this defect. The compressive strain in X and Y directions can be observed for section S3 in Fig. 6 and Fig. 7 respectively. It can be observed that the strain in all sections of all three layers increased over time except in the final layer. The development of warpage in this layer caused shrinkage of the sample as seen in these figures. This trend in strain evolution can be observed in both X and Y directions.

C. Thermal Analysis of Temperature Variation

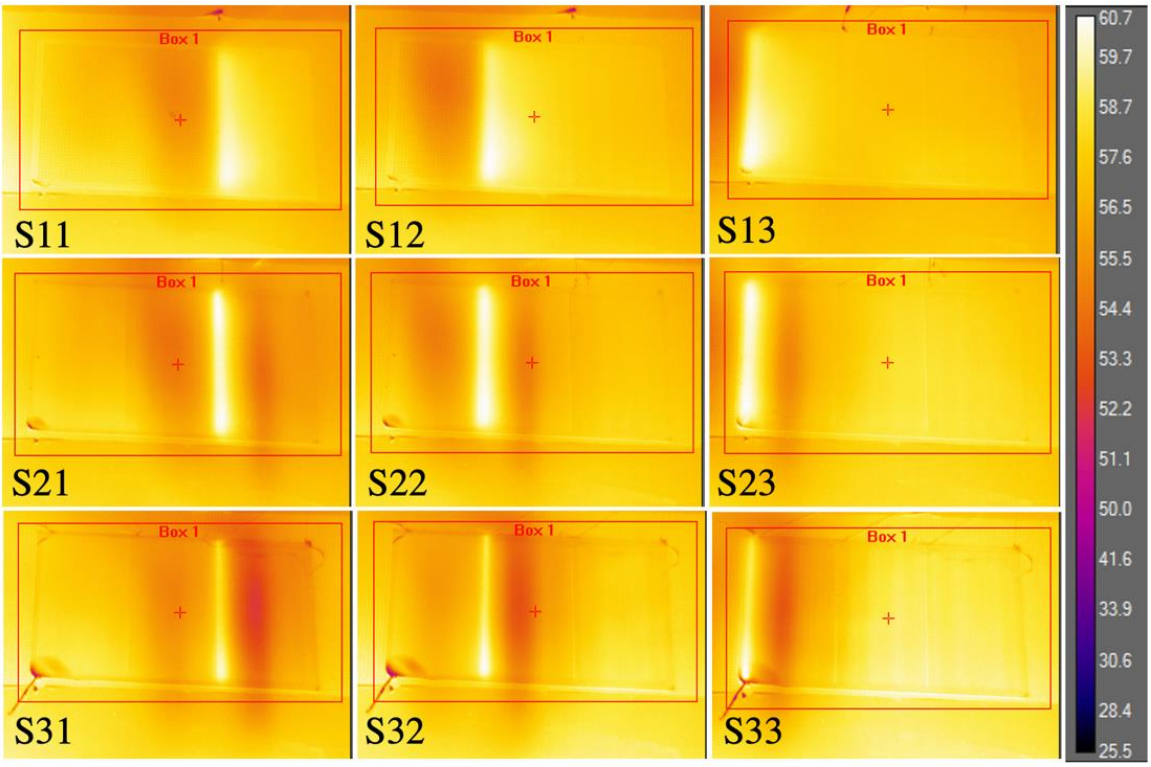

Fig. 8 Thermal images FLIR A655 SC capturing temperature variation

Thermal images of the sample while printing using an infrared (IR) camera can be seen in Figure 8. The IR camera is used to capture the temperature contours of the specimen in real-time every 2.5 minutes. An algorithm similar to the printing algorithm was developed to measure temperature evolution with time for all the sections of the sample. These thermal images derived from the Research IR software of the IR camera are imported into MATLAB as temperature data files. MATLAB was used to process image files and extract average temperature data along the X direction by selecting various lines for each section. Fig. 8 depicts each section printed and the change in temperature along the newly printed edge of each section. Figure 9 shows the temperature distribution across the length of the specimen. The solid line in this figure indicates temperature variation for section 1, the dotted line indicates temperature variation for section 1 and section 2 and the broken line indicates the temperature distribution for sections 1, 2, and 3 together (one complete layer). It can be observed that the freshly printed filament temperature is higher for all the sections. The temperature of the new layer is higher than the previously printed layer as this older layer is

cured and cooled. A maximum temperature variation of 4ºC is observed considering all three layers with a maximum temperature of 59.63 °C and a minimum of 55.72°C. This thermal analysis can be combined with continuous strain evolution to identify the defect initiation point along with the thermal and chemical conditions that contributed to the defect formation.

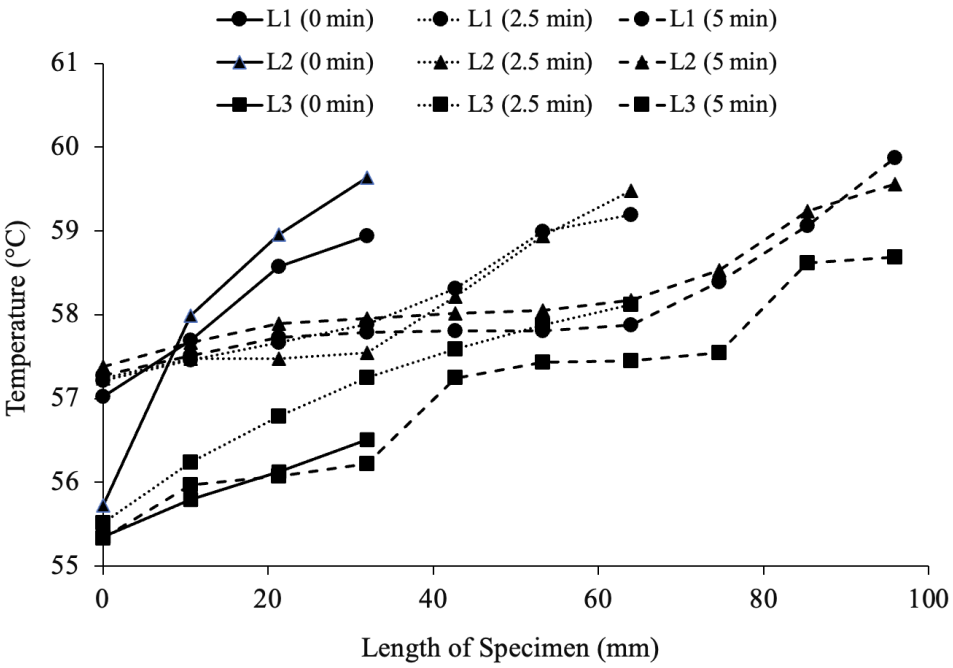

Fig. 9 Temperature variation in the sample over a time of 5 minutes

V. Summary

In summary, a novel in-situ experimental approach using Digital Image Correlation (DIC) is developed to monitor additive manufacturing in real-time. A Marble PLA filament with the black and white pattern as speckle pattern is chosen to be used with Creality Ender 5 Plus 3D printer to print the specimen in this research. Thermal analysis using FLIR A655 SC thermal camera is performed during processing to capture the temperature and cooling rate of part in real-time. A print algorithm has been developed and implemented which divides each layer of the rectangular specimen (96mm*60mm) into three sections allowing surveillance of the progression of defect formation throughout the layer. In-situ strain analysis demonstrates the potential of DIC for in-situ monitoring of additive manufacturing. Discrepancies in strain evolution indicate printing defects such as under extrusion and warping. These strains could be used to estimate residual stresses during processing. The research approach developed in this paper can be used to improve the manufacturing process of additive manufacturing by developing approaches that use the in-situ data and dynamically adjust printing to avoid processing defects.

Acknowledgments

This research was supported by NSF Advanced Manufacturing through grant number 2001038.

References

[1] Wong, K. V, and Hernandez, A. “A Review of Additive Manufacturing.” *International scholarly research notices*, Vol. 2012, 2012.

[2] Ford, S., and Despeisse, M. “Additive Manufacturing and Sustainability: An Exploratory Study of the Advantages and Challenges.” *Journal of cleaner Production*, Vol. 137, 2016, pp. 1573–1587.

[3] Haq, R. H. A., Marwah, O. M. F., Rahman, M. N. A., Haw, H. F., Abdullah, H., and Ahmad, S. 3D Printer Parameters Analysis for PCL/PLA Filament Wire Using Design of Experiment (DOE). No. 607, 2019, pp.

12001.
[4] Kalender, M., Kılıç, S. E., Ersoy, S., Bozkurt, Y., and Salman, S. Additive Manufacturing and 3D Printer Technology in Aerospace Industry. 2019.
[5] Shapiro, A. A., Borgonia, J. P., Chen, Q. N., Dillon, R. P., McEnerney, B., Polit-Casillas, R., and Soloway, L. "Additive Manufacturing for Aerospace Flight Applications." *Journal of Spacecraft and Rockets*, 2016, pp. 952–959.
[6] Bean, Q. A., Cooper, K. G., Edmunson, J. E., Johnston, M. M., and Werkheiser, M. J. International Space Station (Iss) 3d Printer Performance and Material Characterization Methodology. 2015.
[7] Yan, Q., Dong, H., Su, J., Han, J., Song, B., Wei, Q., and Shi, Y. "A Review of 3D Printing Technology for Medical Applications." *Engineering*, Vol. 4, No. 5, 2018, pp. 729–742.
[8] Pravin, S., and Sudhir, A. "Integration of 3D Printing with Dosage Forms: A New Perspective for Modern Healthcare." *Biomedicine & Pharmacotherapy*, Vol. 107, 2018, pp. 146–154.
[9] Kumar, K. P. A., and Pumera, M. "3D-Printing to Mitigate COVID-19 Pandemic." *Advanced Functional Materials*, Vol. 31, No. 22, 2021, p. 2100450.
[10] Ford, S. L. N. "Additive Manufacturing Technology: Potential Implications for US Manufacturing Competitiveness." *J. Int'l Com. & Econ.*, Vol. 6, 2014, p. 40.
[11] Masuo, H., Tanaka, Y., Morokoshi, S., Yagura, H., Uchida, T., Yamamoto, Y., and Murakami, Y. "Influence of Defects, Surface Roughness and HIP on the Fatigue Strength of Ti-6Al-4V Manufactured by Additive Manufacturing." *International Journal of Fatigue*, Vol. 117, 2018, pp. 163–179.
[12] Holzmond, O., and Li, X. "In Situ Real Time Defect Detection of 3D Printed Parts." *Additive Manufacturing*, Vol. 17, 2017, pp. 135–142.
[13] Altıparmak, S. C., Yardley, V. A., Shi, Z., and Lin, J. "Challenges in Additive Manufacturing of High-Strength Aluminium Alloys and Current Developments in Hybrid Additive Manufacturing." *International Journal of Lightweight Materials and Manufacture*, 2020.
[14] Craeghs, T., Clijsters, S., Kruth, J.-P., Bechmann, F., and Ebert, M.-C. "Detection of Process Failures in Layerwise Laser Melting with Optical Process Monitoring." *Physics Procedia*, Vol. 39, 2012, pp. 753–759.
[15] Kousiatza, C., and Karalekas, D. "In-Situ Monitoring of Strain and Temperature Distributions during Fused Deposition Modeling Process." *Materials & Design*, Vol. 97, 2016, pp. 400–406.
[16] Vanaei, H. R., Shirinbayan, M., Costa, S. F., Duarte, F. M., Covas, J. A., Deligant, M., Khelladi, S., and Tcharkhtchi, A. "Experimental Study of PLA Thermal Behavior during Fused Filament Fabrication." *Journal of Applied Polymer Science*, Vol. 138, No. 4, 2021, p. 49747.
[17] Peters, W. H., and Ranson, W. F. "Digital Imaging Techniques in Experimental Stress Analysis." *Optical engineering*, Vol. 21, No. 3, 1982, p. 213427.
[18] Yoneyama, S., and Murasawa, G. "Digital Image Correlation." *Experimental mechanics*, Vol. 207, 2009.
[19] Kahn-Jetter, Z. L., and Chu, T. C. "Three-Dimensional Displacement Measurements Using Digital Image Correlation and Photogrammic Analysis." *Experimental Mechanics*, Vol. 30, No. 1, 1990, pp. 10–16.
[20] Wang, Y. H., Jiang, J. H., Wanintrudal, C., Du, C., Zhou, D., Smith, L. M., and Yang, L. X. "Whole Field Sheet-metal Tensile Test Using Digital Image Correlation." *Experimental Techniques*, Vol. 34, No. 2, 2010, pp. 54–59.
[21] Górszczyk, J., and Malicki, K. "Application of Digital Image Correlation Method for Road and Railway Material Testing."
[22] Quanjin, M., Rejab, M. R. M., Halim, Q., Merzuki, M. N. M., and Darus, M. A. H. "Experimental Investigation of the Tensile Test Using Digital Image Correlation (DIC) Method." *Materials Today: Proceedings*, Vol. 27, 2020, pp. 757–763.
[23] Ding, L., Lin, J., Min, J., Pang, Z., and Ye, Y. "Necking of Q&P Steel during Uniaxial Tensile Test with the Aid of DIC Technique." *Chinese Journal of Mechanical Engineering*, Vol. 26, No. 3, 2013, pp. 448–453.
[24] Paul, S. K., Roy, S., Sivaprasad, S., and Tarafder, S. "A Simplified Procedure to Determine Post-Necking True Stress–Strain Curve from Uniaxial Tensile Test of Round Metallic Specimen Using DIC." *Journal of Materials Engineering and Performance*, Vol. 27, No. 9, 2018, pp. 4893–4899.
[25] He, Z., Zhang, K., Lin, Y., and Yuan, S. "An Accurate Determination Method for Constitutive Model of Anisotropic Tubular Materials with DIC-Based Controlled Biaxial Tensile Test." *International Journal of Mechanical Sciences*, Vol. 181, 2020, p. 105715.
[26] Zhu, F., Bai, P., Zhang, J., Lei, D., and He, X. "Measurement of True Stress–Strain Curves and Evolution of Plastic Zone of Low Carbon Steel under Uniaxial Tension Using Digital Image Correlation." *Optics and Lasers in Engineering*, Vol. 65, 2015, pp. 81–88.
[27] Chava, S., and Namilae, S. "Continuous Evolution of Processing Induced Residual Stresses in Composites:

An in-Situ Approach." *Composites Part A: Applied Science and Manufacturing*, Vol. 145, 2021, p. 106368. https://doi.org/10.1016/j.compositesa.2021.106368.

[28] Abeykoon, C., Sri-Amphorn, P., and Fernando, A. "Optimization of Fused Deposition Modeling Parameters for Improved PLA and ABS 3D Printed Structures." *International Journal of Lightweight Materials and Manufacture*, Vol. 3, No. 3, 2020, pp. 284–297.

[29] Chacón, J. M., Caminero, M. A., García-Plaza, E., and Núnez, P. J. "Additive Manufacturing of PLA Structures Using Fused Deposition Modelling: Effect of Process Parameters on Mechanical Properties and Their Optimal Selection." *Materials & Design*, Vol. 124, 2017, pp. 143–157.

[30] Kantaros, A., and Karalekas, D. "Fiber Bragg Grating Based Investigation of Residual Strains in ABS Parts Fabricated by Fused Deposition Modeling Process." *Materials & Design*, Vol. 50, 2013, pp. 44–50.

[31] Everton, S. K., Hirsch, M., Stravroulakis, P., Leach, R. K., and Clare, A. T. "Review of In-Situ Process Monitoring and in-Situ Metrology for Metal Additive Manufacturing." *Materials & Design*, Vol. 95, 2016, pp. 431–445.

[32] Chava, S., and Namilae, S. "In Situ Investigation of the Kinematics of Ply Interfaces during Composite Manufacturing." *Journal of Manufacturing Science and Engineering, Transactions of the ASME*, Vol. 143, No. 2, 2021. https://doi.org/10.1115/1.4047740.